RSC Advances

PAPER

View Article Online
View Journal | View Issue

CrossMark click for updates

Cite this: *RSC Adv.*, 2015, **5**, 52019

Hydroiodic acid treated PEDOT:PSS thin film as transparent electrode: an approach towards ITO free organic photovoltaics†

Ashis K. Sarker,‡*[a] Jaehoon Kim,‡[a] Boon-Hong Wee,[b] Hyung-Jun Song,[a] Yeonkyung Lee,[a] Jong-Dal Hong[b] and Changhee Lee*[a]

In this article, we introduce a method for fabricating highly conductive transparent poly(3,4-ethylenedioxythiophene):poly(styrenesulfonate) (PEDOT:PSS) thin nano-structured film by treating the pristine PEDOT:PSS film with concentrated (55%) hydroiodic acid (HI). HI treatment on the pristine PEDOT:PSS film could significantly reduce the film sheet resistance without sacrificing its transparency and other electronic properties, which are highly desirable for transparent conductors. A thin layer of HI treated PEDOT:PSS film (74 nm) has very high transmittance of 90% and a low sheet resistance of 95 ohm sq^{-1}. The sheet resistance of the film can be reduced to 37 ohm sq^{-1} by increasing the film thickness but at the expense of its transparency. The low sheet resistance of the film can be attributed to the increase of polarons density, conformational changes and formation of clusters due to removal of some PSS from PEDOT:PSS particles. The results were confirmed by the UV/VIS/near-IR absorption spectroscopy, atomic force microscopy, X-ray photoelectron spectroscopy and energy-dispersive X-ray spectroscopy. Given the high electrical conductivity of the HI treated PEDOT:PSS film, it was then tested as a transparent organic cathode in a polymer solar cell. This ITO-free solar cell showed superior current generation and charge collection with an efficiency of 5.83%, which is 18 times higher than the cell that used untreated PEDOT:PSS film. We, therefore, envisage this potential fabrication method, which uses HI acid, to be applied on other conjugated polymers to enhance their conducting properties for practical applications.

Received 20th April 2015
Accepted 8th June 2015

DOI: 10.1039/c5ra07136d

www.rsc.org/advances

Published on 08 June 2015. Downloaded by Michigan State University on 27/01/2016 00:51:57.

Introduction

The global optoelectronic device manufacturers for organic solar cells, organic light emitting diodes, organic photodetectors, liquid crystal displays, touch panel displays and lasers have placed great demand on the transparent conductive electrodes (TCEs), which are used mainly for transporting electrons to and from these optoelectronic devices. Indium tin oxide (ITO) is currently the major source of material used for these optoelectronic devices owing to its high transparency and high electrical conductivity.[1] ITO, however, has several disadvantages such as intrinsic mechanical brittleness,[2] due to its inferior ceramic-like properties, low chemical resistance in both acidic and alkaline environments, as well as the bulkiness and non-light weight ITO end-products. An ever increasing cost of ITO due to indium scarcity[3] and the necessity for low temperature processing for flexible electronics have prompted the electronic industries to search for cheaper alternative material for flexible transparent conductors.[4,5]

Many materials, including carbon nanotubes (CNTs),[6–8] graphene,[8–12] ultrathin metal films[13,14] and metal nanowires[15,16] have been explored as potential TCEs, as they all exhibit high transparency across the visible light spectrum. TCEs composed of metallic nanowires suffer from large surface roughness, while CNT films have limitations due to high contact resistances between nanotube bundles. Recently, TCEs made of conducting organic materials have attracted much attention due to their unprecedented advantages involving solution processability, flexibility and light weight.[17] The solution processable conducting organic materials has created a new cost effective avenue for manufacturing cheap and high performance electrode for large area optoelectronic devices.[18] The complex of poly(3,4-ethylenedioxythiophene) (PEDOT) and poly(4-styrenesulfonate) (PSS) is successfully used as TCE due to its high electrical conductivity and excellent transparency in the visible range.[19,20] PEDOT:PSS conducting films consist of hydrophobic and conducting PEDOT-rich grains encapsulated

[a]*Department of Electrical and Computer Engineering, Global Frontier for Multiscale Energy Systems, Seoul National University, Seoul 151-742, Republic of Korea. E-mail: chlee7@snu.ac.kr; ashischemru@gmail.com; Fax: +82-2-877-6668; Tel: +82-2-880-9093*

[b]*Department of Chemistry, Research Institute of Natural Sciences, Incheon National University, 119 Academy-ro, Yeonsu-gu, Incheon, 406-772, Republic of Korea*

† Electronic supplementary information (ESI) available. See DOI: 10.1039/c5ra07136d

‡ These authors have equal contribution in the work.

Published on 08 June 2015. Downloaded by Michigan State University on 27/01/2016 00:51:57.

by hydrophilic and insulating PSS-rich shells.[21] These films have an excess amount of PSS as well as low chain alignment, resulting in low conductivity of approximately 0.2 S cm^{-1}. PSS is used as the counter ion and charge compensator and template for the polymerization of PEDOT hence allowing the PEDOT:PSS particles to be easily dispersed in water. Given that PSS is an insulator, the presence of PSS has been the main reason for the low conductivity of the commercial PEDOT:PSS.[20,22] In order to improve the conductivity of PEDOT:PSS, several methods have been reported including the addition of organic compound, such as ethylene glycol,[19,23] dimethyl sulfoxide,[24,25] ionic liquid,[26,27] anionic surfactant,[28] or dimethyl sulfate,[24] as well as the treatment of PEDOT:PSS films with a polar organic compound,[29] salt,[30,31] sorbitol,[32] zwitterion,[33] carboxylic[34] or inorganic acid,[35,36] or co solvent.[37] Numerous studies suggested that the conductivity enhancement could be attributed to morphological changes in the PEDOT:PSS complex, such as grain growth, polymer chain expansion, and phase separation. However, a clear understanding of the mechanism of the conductivity enhancement of PEDOT:PSS films is still necessary for developing high-performance conjugated polymer-based TCEs.

Here, we report a facile method for enhancing the conductivity of PEDOT:PSS film by treating the as-prepared film with hydroiodic acid (HI). We have first investigated the conductivity enhancement of polyaniline after HI treatment.[38] This enhancement was due to the increase in doping density of the polymer chains.[39] In this work, we have treated PEDOT:PSS film by immersing in HI solution resulting in a highly conductive film that was subsequently used as TCE for polymer solar cell (PSC).

Experimental

Materials

Aqueous PEDOT : PSS solution (1.3 wt%, CLEVIOS™ PH 1000) was purchased from Heraeus Precious Metals Gmbh & Co. KG, and the weight ratio of PSS to PEDOT was 2.5. Hydroiodic acid (HI, 55%), zinc acetate ($Zn(CH_3COO)_2 \cdot 2H_2O$) and potassium hydroxide (KOH) were purchased from Sigma-Aldrich. Poly({4,8-bis[(2-ethylhexyl)oxy]benzo[1,2-b:4,5-b′]dithiophene-2,6-diyl}{3-fluoro-2-[(2-ethylhexyl)carbonyl]thieno[3,4-b]thiophenediyl}) (PTB7) and phenyl-C71-butyric acid methyl ester ($PC_{71}BM$) were purchased from 1-Material Inc. Ultrapure water (Water purification system, Human Power I+) was used for all experiments including the preparation of acid solutions, and cleaning steps.

Electrode preparation

Glass substrate of area 2.4 × 2.0 cm^2 was cleaned successively ultra-sonicating in acetone, isopropyl alcohol and deionized water for 30 min per each treatment, and then dried in an oven at 120 °C in ambient condition. PEDOT:PSS filtered through a 1.0 μm size filter was spin-coated at 2000 rpm for 40 s on a cleaned glass substrate that was pretreated 10 min with UV/ozone plasma. The substrate coated with PEDOT:PSS was then annealed on a hot plate in the ambient condition at 120 °C for 10 min to remove the residual amount of water. Then, PEDOT:PSS film was immersed in HI (55%) for 30 min. Subsequently, the PEDOT:PSS film was washed with acetone and deionized water to remove residual HI prior to drying at 120 °C for 60 min. The HI treated film was highly stable during the washing step, while as-prepared film was washed away from the glass substrate (Fig. S1 and S2†). Note that thick PEDOT:PSS film was prepared by repeating the whole processes sequentially.

Synthesis of ZnO nanoparticles

ZnO nanoparticle suspensions (dispersed into butanol) were prepared by a method reported previously.[40] In brief, the mixture of $Zn(CH_3COO)_2 \cdot 2H_2O$ (2 g) and methanol (80 ml) was heated to 60 °C. After the stabilization of the solution temperature at 60 °C, KOH solution (1.51 g in 65 ml in methanol) was added dropwise into the mixture, and then stirred for 145 min. ZnO nanoparticles formed in the mixture were isolated by centrifugation at 4000 rpm, and re-dispersed in 1-butanol, resulting in the concentration of 20 mg ml^{-1}. The ZnO nanoparticle size was estimated around 5 ± 1 nm by transmission electron microscopy (JEM1010, JEOL) shown in the ESI (Fig. S3†).

Device fabrication

The PEDOT:PSS film electrode was first patterned by 250 nm thick SiO_x, which was selectively deposited on it using a vacuum thermal evaporation technique. Subsequently, ZnO nanoparticles were spin-coated on the patterned PEDOT:PSS film electrode at 2000 rpm for 40 s, which were then dried in N_2 oven at 90 °C for 30 min. Polymer blend was prepared as a photoactive layer by dissolving PTB7 : PCBM (1 : 1.5 by weight ratio) into a mixture solvent composed of chlorobenzene (CB)/1,8-diiodooctane (DIO) (97 : 3 by volume%), yielding a total concentration of 25 mg ml^{-1}. Photoactive layer was deposited on top of ZnO nanoparticle layer of the patterned PEDOT:PSS film electrode by spin-coating the polymer blend at 1000 rpm for 30 s. Then, photoactive layer was dried slowly in vacuum overnight, and fabricated with MoO_x (10 nm)/Al (100 nm) in the deposition rate of 0.23 and 2.3 Å s^{-1}, respectively. The active area of the device was 1.4 × 1.4 mm^2.

Measurements

The current density (*J*–*V*) characteristics was measured using Keithley 237 source measurement unit with AM 1.5G solar simulator (Newport, 91160A). The sheet resistance of the PEDOT:PSS film was determined using four point probe (Changmin Co., Ltd.). The transmittance and absorption spectra were recorded by a UV/visible spectrophotometer (Beckman Coulter, US/DU 7000 Series). Surface morphology characterization and thickness measurement of PEDOT:PSS film was performed using atomic force microscopy (AFM) (Park Systems, XE-100). Spectroscopic analysis of PEDOT:PSS film surface was performed by using X-ray photoelectron spectroscopy (XPS) (Kratos Analytical Ltd) and energy-dispersive X-ray spectroscopy (EDS) (Carl Zeiss AG), respectively.

 This journal is © The Royal Society of Chemistry 2015

Published on 08 June 2015. Downloaded by Michigan State University on 27/01/2016 00:51:57.

Results and discussion

The thickness of one-layer spin-coated PEDOT:PSS film was found to reduce from 53 nm to 39 nm after HI treatment, as measured from AFM. The thickness of the PEDOT:PSS film can be increased linearly by repeating the spin coating step followed by HI treatment. Therefore, two-layer HI-treated PEDOT:PSS film thickness was measured to be 74 nm, approximately two times the thickness of the one-layer HI-treated PEDOT:PSS film. This was found to be the optimized film thickness for fabricating high performance device. The conductivity of the pristine PEDOT:PSS film (~0.2 S cm^{-1}) increased by four orders of magnitude to over 1100 S cm^{-1} after HI treatment.

Fig. 1a depicts the transmittance in the visible range of pristine and HI treated PEDOT:PSS film of different thicknesses. A one-layer PEDOT:PSS film before and after HI treatment exhibited a transmittance more than 90% over the whole wavelength range of 400–800 nm. As expected, the transmittance for a two-layer PEDOT:PSS film was observed to decrease slightly. A decrease in the transmittance for the HI-treated two-layer film can be clearly seen particularly in the higher wavelength (>550 nm) region. The transmittance for a three-layer PEDOT:PSS film particularly in the low wavelength region still remained above 90% but it fell gradually below 80% in the higher wavelength region (>700 nm). The spectra for HI-treated film obviously exhibited an interesting pattern in that its transmittance was observed to be higher in the low wavelength region (400–600 nm) but lower in the high wavelength region (>700 nm), as compared with the transmittance spectra for the pristine three-layer film.

Since the transmittance and sheet resistance are two interesting parameters that govern the overall performance of the optoelectronic devices, it is therefore worthwhile to study these parameters in detail. We observed a sheet resistance of 95 ohm sq^{-1} on HI treated two-layer PEDOT:PSS films which had a transmittance of 92% in the visible range. The sheet resistance decreased to 37 ohm sq^{-1} for HI treated five-layer PEDOT:PSS films, however, the transmittance of film was reduced to about 72% at 550 nm. It is notable that the successive film deposition decrease the sheet resistance (desirable) while reduces the transmittance (undesirable) (Table S1†). This sheet resistance (37 ohm sq^{-1}) is lower than that of the ITO coated on polyethylene terephthalate, having a typical sheet resistance of 50 ohm sq^{-1}. This highly reproducible and straightforward fabrication method could produce over 100 samples with minimal sample-to-sample variation in terms of their sheet resistance. In addition, the HI treated PEDOT:PSS films have good stability in terms of sheet resistance and transparency. Fig. 1a (inset) presents a photographic image of the HI treated PEDOT:PSS film (sheet resistance = 95 ohm sq^{-1}) on a glass substrate insinuating its excellent transparency to visible light.

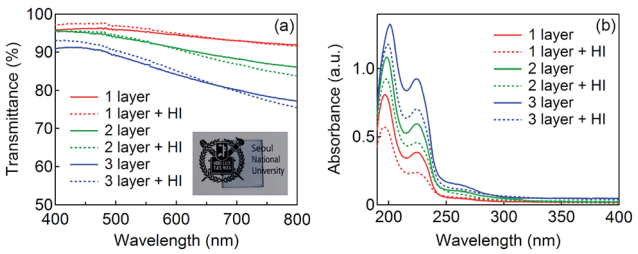

Fig. 1 (a) Transmittance spectra and (b) UV absorption spectra of single, double, and triple layered PEDOT:PSS films before and after HI treatment.

The influence of the HI-treatment on spectral states of the PEDOT:PSS films in 190–400 nm region was investigated through comparison with those of the pristine films in the single, double and triple layers, as shown in Fig. 1b. Note that the characteristic absorption bands at 200 and 225 nm are originated from the aromatic ring of PSS in PEDOT:PSS films. The HI treatment of the three different PEDOT:PSS films led to the decrease in their absorption intensities of the peaks at 200 and 225 nm. The outcome of this study indicated that PSS involved in shell was washed out from PEDOT:PSS film electrodes during the HI treatments. This interpretation of the results was strengthened by the fact that there was no significant change of the spectral features in visible region, which were responsible for the absorbance of PEDOT. An additional evidence for the partial desorption of PSS in shell was the weak increase in hydrophobicity of pristine PEDOT:PSS films from 34° to 41° as determined using the water contact angle measurement (Fig. S4†). Note that the increased film hydrophobicity did not cause any significant problem for the deposition of ZnO buffer layer followed by the PEDOT:PSS coating.

The influence of the HI treatment on the surface morphology of the pristine PEDOT:PSS film was analyzed based on the topographical AFM images, as shown in Fig. 2. The surface roughness of the pristine PEDOT:PSS film increased from 1.44 to 1.82 nm after the HI treatment. However, no significant morphological changes was found on the PEDOT:PSS film after the HI treatment except the formation of small domains (Fig. 2b). The small domains are corresponded to PEDOT:PSS granules, which exist in core/shell structure in water and in the as-prepared film, as reported in detail previously.[41] The core of PEDOT:PSS granules is rich of conductive PEDOT, whereas the shell is rich of nonconductive PSS. The confirmation of these granules (in core/shell structure) supported the improvement in the conductivity of PEDOT:PSS film electrodes through the desorption of PSS in shell during the HI treatment, which could also be confirmed by the spectral investigation. The decrease of the shell thickness *via* desorption of nonconductive PSS component seems to lower the energy barrier for the inter-chain and inter-domain charge hopping, resulting in drastic conductivity enhancement for PEDOT:PSS film electrodes.

The chemical composition of PEDOT:PSS film was analyzed by using X-ray photoelectron spectroscopy (XPS) (Fig. 3). A high-resolution XPS survey scan of PEDOT:PSS film before and after HI treatment showed three distinct peaks corresponding to O 1s (532), C 1s (284), and S 2p (168). The absence of strong iodine peaks at 630 and 619 eV (ref. 42) in the XPS spectra of HI-treated PEDOT:PSS film indicated that the HI residue was completely removed from the film electrode during the post cleaning steps (Fig. 3a and S5†). High-resolution S 2p spectra of PEDOT:PSS film before and after HI treatment (Fig. 3b) was utilized to

Published on 08 June 2015. Downloaded by Michigan State University on 27/01/2016 00:51:57.

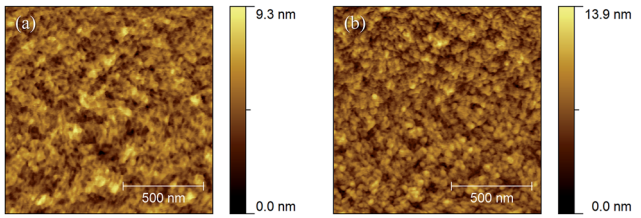

Fig. 2 AFM topographical images of (a) pristine and (b) HI treated PEDOT:PSS films.

estimate the composition of PEDOT and PSS in those films. The two XPS bands with binding energy between 166 and 172 eV originate from the sulfur atoms in PSS, whereas the two XPS bands with binding energy between 162 to 166 eV are due to the sulfur atoms in PEDOT.[43] There was a clear decrease in the normalized intensity of S 2p peaks based on PSS unlike the case of PEDOT after the HI treatment. Again, the result of the analysis indicated that PSS was mainly desorbed from PEDOT:PSS films during the HI treatment. The molar ratio of PSS to PEDOT in a PEDOT:PSS film decreased from 2.61 to 1.65 after the HI treatment. The decreased value corresponds to 37% of PSS in pristine complex film, whereby the ratio of PEDOT to PSS was calculated using the integral area of the de-convoluted peaks assigned to PEDOT and PSS, respectively.

High conductivities achieved from the doped conducting polymers are associated with formation of self-localized excitations such as solitons, polarons and bipolarons, which may move rather freely through the material. The doping level of the HI treated PEDOT:PSS films was investigated using VIS/NIR absorption spectrometry, as shown in Fig. 4. The absorbance of the PEDOT:PSS films increased significantly over the wavelengths ranging from 700 to 1200 nm after HI treatment. The optical transition at this range corresponds to both polarons or uncoupled bipolarons transitions associated with benzoid/quinoid structure.[44] The strong increase of absorbance in NIR region indicated the density of polarons/uncoupled bipolarons enhanced after HI treatment due to redox reactions in PEDOT polymer chains with HI.

The conductivity increment of PEDOT:PSS films after acid treatment was previously explained by the removal of PSS as PSSH with the help of acid anion.[43] In this work, we have observed a relatively smaller fraction of PSS removed from shells (37%) by HI treatment compared to other acids or

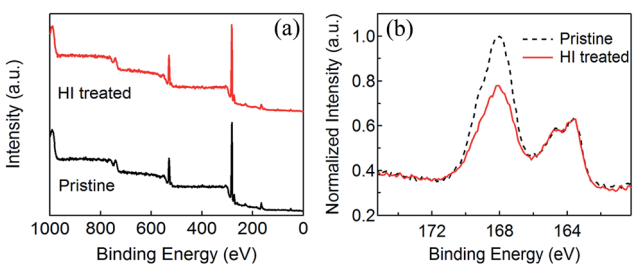

Fig. 3 X-ray photoelectron spectra of pristine and HI treated PEDOT:PSS films. (a) Survey scan, (b) S 2p de-convolution.

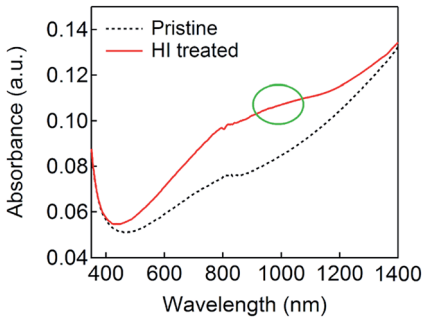

Fig. 4 Visible/NIR absorption spectra of pristine and HI treated PEDOT:PSS films.

solvents treatment (70%).[45,46] Therefore, it is necessary to elucidate the conduction mechanism involved in HI treated PEDOT:PSS films. HI will undergo oxidation, if left to open air according to the following pathways (1) and (2):[47]

$$4HI + O_2 \rightarrow 2H_2O + 2I_2 \quad (1)$$

$$HI + I_2 \rightarrow HI_3 \quad (2)$$

HI_3 is dark brown in color, and dissociates into H^+ and I_3^-. Triiodide ion can accept electron from the PEDOT chain and stabilize as I^- ion due to the thermodynamic stability of oxidized PEDOT chain. While PEDOT:PSS is treated by HI, H^+ (dissociated from HI) will associate with PSS^-, the counter anion of positively charged PEDOT in the PEDOT:PSS, resulting in the formation of PSSH, which is removed from shells. This interpretation was supported by the fact that the pK_a value of HI (−9.3) is higher than the pK_a value of PSSH (−2.8). The complete reaction is proposed as $HI + PSS^- \rightarrow I^- + PSSH$. Now, the PSSH chain is neutral in charge, and does not have Columbic interactions with PEDOT, resulting in phase separation between the hydrophilic PSSH and hydrophobic PEDOT chains, which eases the removal of PSSH from shell.

To test the performance of HI treated PEDOT:PSS film as electrode, PSC is fabricated using them as a transparent cathode with a device architecture as shown in Fig. 5a. The molecular structure of donor (PTB7) and acceptor ($PC_{71}BM$) has been shown in Fig. 5b. The energy level diagram shown in Fig. 5c shows the exciton dissociation at the donor/acceptor interface and the flow of charge carriers (e and h) towards their respective electrodes. For comparison, PSC is also fabricated over pristine PEDOT:PSS film. *J–V* characteristics of the PSC with pristine, HI treated PEDOT:PSS and ITO as cathode are measured (Fig. 5d). It is apparent from the *J–V* characteristics of PSCs that both the short-circuit current density (J_{SC}) and open circuit voltage (V_{OC}) has increased for the PSC with HI treated PEDOT:PSS. The value of J_{SC} has increased from 2.02 to 11.62 mA cm^{-2} while V_{OC} has increased from 0.60 to 0.76 V. Increase in J_{SC} is the direct consequence of the higher conductivity of HI treated PEDOT:PSS film in comparison to the pristine ones. While the increase in V_{OC} can be ascribed to the improvement of interface of photoactive layer with HI treated PEDOT:PSS in

 This journal is © The Royal Society of Chemistry 2015

Published on 08 June 2015. Downloaded by Michigan State University on 27/01/2016 00:51:57.

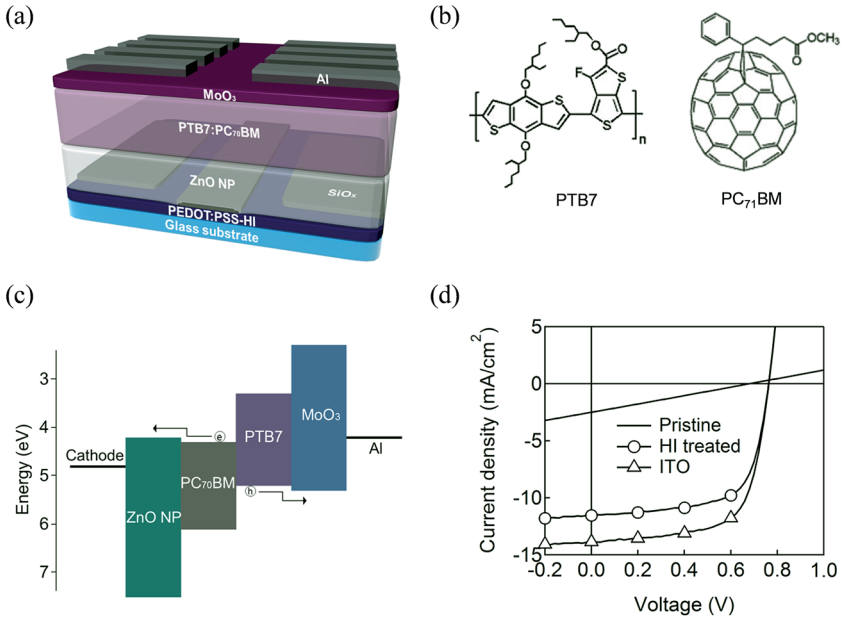

Fig. 5 (a) Device architecture of a polymer solar cell with a HI treated PEDOT:PSS film as the transparent cathode. (b) Schematic representation of PTB7 and $PC_{71}BM$. (c) Energy level diagram of the solar cells. (d) Comparison of the J–V characteristics of polymer solar cells with pristine, HI treated PEDOT:PSS and ITO cathode.

comparison to that with the pristine PEDOT:PSS. It is observed by Mihailetchi *et al.*[48] that V_{OC} of a bulk hetero-junction OPV ([6,6]-phenyl C61-butyric acid methyl ester (PCBM) as electron acceptor and poly[2-methoxy-5-(3′,7′-dimethyloctyloxy)-*p*-phenylene vinylene] (OC1C10-PPV)) is dependent on the electrode if the one of the contact (cathode in their study) is non-ohmic and they observed a V_{OC} value of 0.59 eV when Au is used as a cathode while this value changed to 0.674 and 0.902 V for Ag and LiF/Al as cathode. The increase is ascribed as a better contact formation in case of LiF/Al in comparison to Ag and Au. However, once an ohmic contact is formed the value of V_{OC} becomes independent of electrode and solely determined by the difference between HOMO value of donor and LUMO value of acceptor. In our case, a low conductivity PEDOT:PSS may yield to a non-ohmic contact at PEDOT:PSS/ZnO interface. As the conductivity has increased after HI treatment, the contact has improved which may be the reason behind the increase in V_{OC}. Fill factor (FF) has noticeably increased from 25.23% to 65.60%, which is combined result of the improved electron extraction layer/cathode interfacial contact and resistance between the cathode and electron extraction layer. Combined increase of J_{SC}, V_{OC} and FF in case of PSC with HI treated PEDOT:PSS film as cathode yielded a power conversion efficiency (η) of 5.83%, which was nearly 18 times higher compared with pristine PEDOT:PSS (η = 0.31%) (Table 1). The photovoltaic performance of the ITO device is: J_{SC} of 13.70 mA cm^{-2}, V_{OC} of 0.76 V, FF of 67.24% and efficiency of 7.0%. The value of efficiency of the HI treated PEDOT:PSS device is around 84% of the ITO device (Table 1), close to those previous reports.[49,50]

In this work, we have improved the electron conductivity of PEDOT:PSS films using HI treatment similar to as reported by addition of dimethyl sulfate (DMS) by Reyes-Reyes *et al.*[51]

Table 1 Photovoltaic parameters and efficiencies of polymer PVs with pristine, HI treated PEDOT:PSS and ITO films as the cathode

Sample	J_{SC} (mA cm^{-2})	V_{OC} (V)	FF (%)	PCE (%)
Pristine	2.02 ± 0.49	0.60 ± 0.12	25.23 ± 0.11	0.31 ± 0.12
HI treated	11.62 ± 0.08	0.76 ± 0.00	65.60 ± 1.35	5.83 ± 0.06
ITO	13.70 ± 0.16	0.76 ± 0.00	67.24 ± 0.45	7.00 ± 0.12

(Table S2†). Photovoltaic performance very close to ITO as electrode is achieved by using HI treated PEDOT:PSS as electrode. Therefore, the work also provides an alternative to ITO in case of inverted photovoltaic structure. PEDOT:PSS has been widely used by now as an hole transport layer and has become an integral part of current OPV structure. Improving its electron conductivity makes it a versatile element for future OPV research. It has already been reported that DMS treatment improves the electron conductivity. Current work provides additional treatment choice for improving its electron conductivity. And a consequent test for photovoltaic performance proves that electron conductivity is significantly improved.

Conclusions

A facile method that involves the concentrated (55%) HI treatment on the pristine PEDOT:PSS films is reported, which has significantly enhanced the conductivity of the PEDOT:PSS films from 0.2 S cm^{-1} to over 1100 S cm^{-1}. We proposed that the conductivity enhancement was originated from the increase in the polarons density, conformational changes and formation of clusters due to removal of some PSS from PEDOT:PSS particles. The results were confirmed by the UV/VIS/NIR absorption, AFM,

Published on 08 June 2015. Downloaded by Michigan State University on 27/01/2016 00:51:57.

XPS and EDS spectroscopy. This highly conductive HI treated PEDOT:PSS film was used as the transparent cathode in PSC that has exhibited promising performance with power conversion efficiency as high as 5.83%. This work will add up to the existing knowledge on conductivity enhancement of PEDOT:PSS and opens up new insights to further boost its conductivity.

Acknowledgements

This work was financially supported by the Korea Ministry of Science, ICT & Future through the Global Frontier R&D Program on Center for Multiscale Energy System (2011-0031561) and the Human Resources Development Program of the Korea Institute of Energy Technology Evaluation and Planning (KETEP) grant funded by the Korea government Ministry of Knowledge Economy (no. 20124010203170). We thank Dr Priyanka Tyagi for her valuable suggestions in this work.

References

1 H. Kim, C. M. Gilmore, A. Piqué, J. S. Horwitz, H. Mattoussi, H. Murata, Z. H. Kafafi and D. B. Chrisey, *J. Appl. Phys.*, 1999, **86**, 6451–6461.
2 K. A. Sierros, N. J. Morris, K. Ramji and D. R. Cairns, *Thin Solid Films*, 2009, **517**, 2590–2595.
3 A. Feltrin and A. Freundlich, *Renewable Energy*, 2008, **33**, 180–185.
4 B. G. Lewis and D. C. Paine, *MRS Bull.*, 2000, **25**, 22–27.
5 O. Inganas, *Nat. Photonics*, 2011, **5**, 201–202.
6 Y. H. Kim, L. Müller-Meskamp, A. A. Zakhidov, C. Sachse, J. Meiss, J. Bikova, A. Cook, A. A. Zakhidov and K. Leo, *Sol. Energy Mater. Sol. Cells*, 2012, **96**, 244–250.
7 A. Kaskela, A. G. Nasibulin, M. Y. Timmermans, B. Aitchison, A. Papadimitratos, Y. Tian, Z. Zhu, H. Jiang, D. P. Brown, A. Zakhidov and E. I. Kauppinen, *Nano Lett.*, 2010, **10**, 4349–4355.
8 D. S. Hecht, L. Hu and G. Irvin, *Adv. Mater.*, 2011, **23**, 1482–1513.
9 S. Bae, H. Kim, Y. Lee, X. Xu, J.-S. Park, Y. Zheng, J. Balakrishnan, T. Lei, H. Ri Kim, Y. I. Song, Y.-J. Kim, K. S. Kim, B. Ozyilmaz, J.-H. Ahn, B. H. Hong and S. Iijima, *Nat. Nanotechnol.*, 2010, **5**, 574–578.
10 Y. Wang, S. W. Tong, X. F. Xu, B. Özyilmaz and K. P. Loh, *Adv. Mater.*, 2011, **23**, 1514–1518.
11 Z. Liu, J. Li, Z.-H. Sun, G. Tai, S.-P. Lau and F. Yan, *ACS Nano*, 2011, **6**, 810–818.
12 Z. Liu, J. Li and F. Yan, *Adv. Mater.*, 2013, **25**, 4296–4301.
13 S. Schubert, J. Meiss, L. Müller-Meskamp and K. Leo, *Adv. Energy Mater.*, 2013, **3**, 438–443.
14 D. S. Ghosh, L. Martinez, S. Giurgola, P. Vergani and V. Pruneri, *Opt. Lett.*, 2009, **34**, 325–327.
15 J.-Y. Lee, S. T. Connor, Y. Cui and P. Peumans, *Nano Lett.*, 2008, **8**, 689–692.
16 C. Sachse, L. Müller-Meskamp, L. Bormann, Y. H. Kim, F. Lehnert, A. Philipp, B. Beyer and K. Leo, *Org. Electron.*, 2013, **14**, 143–148.
17 S. R. Forrest, *Nature*, 2004, **428**, 911–918.
18 J. Heeger, N. S. Sariciftci and E. B. Namdas, *Semiconducting and Metallic Polymers*, Oxford University Press Inc., New York, 2010, p. 278.
19 Y. H. Kim, C. Sachse, M. L. Machala, C. May, L. Müller-Meskamp and K. Leo, *Adv. Funct. Mater.*, 2011, **21**, 1076–1081.
20 L. Groenendaal, F. Jonas, D. Freitag, H. Pielartzik and J. R. Reynolds, *Adv. Mater.*, 2000, **12**, 481–494.
21 U. Lang, E. Müller, N. Naujoks and J. Dual, *Adv. Funct. Mater.*, 2009, **19**, 1215–1220.
22 S. Kirchmeyer and K. Reuter, *J. Mater. Chem.*, 2005, **15**, 2077–2088.
23 D. Alemu Mengistie, P.-C. Wang and C.-W. Chu, *J. Mater. Chem. A*, 2013, **1**, 9907–9915.
24 M. Reyes-Reyes, I. Cruz-Cruz and R. López-Sandoval, *J. Phys. Chem. C*, 2010, **114**, 20220–20224.
25 J. Y. Kim, J. H. Jung, D. E. Lee and J. Joo, *Synth. Met.*, 2002, **126**, 311–316.
26 M. Döbbelin, R. Marcilla, M. Salsamendi, C. Pozo-Gonzalo, P. M. Carrasco, J. A. Pomposo and D. Mecerreyes, *Chem. Mater.*, 2007, **19**, 2147–2149.
27 C. Badre, L. Marquant, A. M. Alsayed and L. A. Hough, *Adv. Funct. Mater.*, 2012, **22**, 2723–2727.
28 B. Fan, X. Mei and J. Ouyang, *Macromolecules*, 2008, **41**, 5971–5973.
29 J.-H. Huang, D. Kekuda, C.-W. Chu and K.-C. Ho, *J. Mater. Chem.*, 2009, **19**, 3704–3712.
30 Y. Xia and J. Ouyang, *Org. Electron.*, 2010, **11**, 1129–1135.
31 Y. Xia and J. Ouyang, *Macromolecules*, 2009, **42**, 4141–4147.
32 A. M. Nardes, M. Kemerink, M. M. de Kok, E. Vinken, K. Maturova and R. A. J. Janssen, *Org. Electron.*, 2008, **9**, 727–734.
33 Y. Xia, H. Zhang and J. Ouyang, *J. Mater. Chem.*, 2010, **20**, 9740–9747.
34 Y. Xia and J. Ouyang, *ACS Appl. Mater. Interfaces*, 2010, **2**, 474–483.
35 I. Cruz-Cruz, M. Reyes-Reyes and R. López-Sandoval, *Thin Solid Films*, 2013, **531**, 385–390.
36 R. M. Howden, E. D. McVay and K. K. Gleason, *J. Mater. Chem. A*, 2013, **1**, 1334–1340.
37 Y. Xia and J. Ouyang, *J. Mater. Chem.*, 2011, **21**, 4927–4936.
38 A. K. Sarker and J.-D. Hong, *Langmuir*, 2012, **28**, 12637–12646.
39 A. K. Sarker and J.-D. Hong, *Colloids Surf., A*, 2013, **436**, 967–974.
40 W. K. Bae, Y.-S. Park, J. Lim, D. Lee, L. A. Padilha, H. McDaniel, I. Robel, C. Lee, J. M. Pietryga and V. I. Klimov, *Nat. Commun.*, 2013, **4**, 1–8.
41 Y. H. Kim, C. Sachse, M. L. Machala, C. May, L. M. Meskamp and K. Leo, *Adv. Funct. Mater.*, 2011, **21**, 1076–1081.
42 A. K. Sarker and J.-D. Hong, *Bull. Korean Chem. Soc.*, 2014, **35**, 1799–1805.
43 Y. Xia, K. Sun and J. Ouyang, *Adv. Mater.*, 2012, **24**, 2436–2440.
44 M. Nowak, S. D. D. V. Rughooputh, S. Hotta and A. J. Heeger, *Macromolecules*, 1987, **20**, 965–968.

 This journal is © The Royal Society of Chemistry 2015

45 N. Kim, S. Kee, S. H. Lee, B. H. Lee, Y. H. Kahng, Y.-R. Jo, B.-J. Kim and K. Lee, *Adv. Mater.*, 2014, **26**, 2268–2272.
46 D. A. Mengistie, M. A. Ibrahem, P.-C. Wang and C.-W. Chu, *ACS Appl. Mater. Interfaces*, 2014, **6**, 2292–2299.
47 P. H. Svensson and L. Kloo, *Chem. Rev.*, 2003, **103**, 1649–1684.
48 V. D. Mihailetchi, P. W. M. Blom, J. C. Hummelen and M. T. Rispens, *J. Appl. Phys.*, 2003, **94**, 6849.
49 Y. Zhou, H. Cheun, S. Choi, W. J. Potscavage, C. F. Hernandez and B. Kippelen, *Appl. Phys. Lett.*, 2010, **97**, 153304.
50 Y. Xia, K. Sun and J. Ouyang, *Energy Environ. Sci.*, 2012, **5**, 5325.
51 M. Reyes-Reyes, I. Cruz-Cruz and R. Lopez-Sandoval, *J. Phys. Chem. C*, 2010, **114**, 20220–20224.

Published on 08 June 2015. Downloaded by Michigan State University on 27/01/2016 00:51:57.